Ecosystems (2009) 12: 517–533
DOI: 10.1007/s10021-009-9238-4

ECOSYSTEMS


# Modeling the Sensitivity of the Seasonal Cycle of GPP to Dynamic LAI and Soil Depths in Tropical Rainforests

Benjamin Poulter,[1]* Ursula Heyder,[1] and Wolfgang Cramer[1,2]

[1]*Earth System Analysis, Potsdam Institute for Climate Impact Research (PIK), Telegraphenberg A26, Potsdam 14412, Germany;*
[2]*Centre Européen de Recherche et d'Enseignement des Géosciences de l'Environnement (CEREGE), BP 80, 13545 Aix-en-Provence cedex 04, France*

## Abstract

The seasonality of pan-tropical wet forests has been highlighted by recent remote sensing and eddy flux measurements that have recorded both increased and sustained dry-season gross primary productivity (GPP). These observations suggest that wet tropical forests are primarily light limited and that the mechanisms for resilience to drought and projected climate change must be considered in ecosystem model development. Here we investigate two proposed mechanisms for drought resilience of tropical forests, deep soil water access and the seasonality of phenology, using the LPJmL Dynamic Global Vegetation Model. We parameterize a new seasonal phenology module for tropical evergreen trees using remotely sensed leaf area index (LAI) and incoming solar radiation data from the Terra Earth Observing System. Simulations are evaluated along a gradient of dry-season length (DSL) in South America against MODIS GPP estimates. We show that deep soil water access is critical for maintaining dry-season GPP, whereas implementing a seasonal LAI did not enhance simulated dry-season GPP. The Farquhar-Collatz photosynthesis scheme used in LPJmL optimizes leaf nitrogen allocation according to light conditions, causing maximum photosynthetic capacity in the dry season. High LAI, characteristic of tropical forests, also dampens the seasonal amplitude of the fraction of photosynthetically active radiation (FPAR). Given the relatively high uncertainty in tropical phenology observations and their corresponding proximate drivers, we recommend that ecosystem model development focus on belowground processes. An improved representation of soil depths and rooting distributions is necessary for modeling the dynamics of dry-season tropical forest functioning and may have important impacts for modeling tropical forest vulnerability to climate change.

**Key words:** drought; ecosystem processes; LPJmL; MODIS; $V_{cmax}$; photosynthesis.

Received 13 June 2008; accepted 19 January 2009;
published online 10 March 2009
**Author Contributions**: BP conceived of the study, analyzed data, and wrote the paper. UH designed study and contributed new methods. WC designed study and contributed to paper.

**Corresponding author; e-mail:* Ben.Poulter@pik-potsdam.de

## Introduction

### Drought Sensitivity of Wet Tropical Forests

The wet tropical forests of the Amazon basin are vulnerable to both short and long-term threats that

include deforestation, periodic drought, and climate change (Cramer and others 2004; Malhi and others 2008). Climate change may permanently alter the types of ecosystems supported in the region, initiated through a process of large-scale forest 'dieback' resulting from reduced rainfall projected for the latter half of the 21st century (Cox and others 2004). It is unclear, however, how sensitive tropical ecosystems are to changing temperature and precipitation regimes: the paleo-record suggests relatively high-resilience to millennial-scale climate change (Mayle and Power 2008), whereas ecosystem models show a range of responses to future climate change (Salazar and others 2007).

Recent observations from the Moderate Resolution Imaging Spectroradiometer (MODIS) sensor suggest that wet Amazon forests are primarily light- rather than water-limited (Huete and others 2006; Myneni and others 2007; Saleska and others 2007). Various mechanisms have been proposed to maintain tropical forest functioning during dry-periods and these suggest an increase in forest resilience to projected climate change (Saleska and others 2007). A range of measurements, from eddy covariance (Keller and others 2004), remote sensing (Myneni and others 2007) and atmospheric inversion models (Rödenbeck and others 2003) have converged to highlight the importance of dry-season biogeochemistry and its influence on energy, water and carbon fluxes. This biogeochemical activity is considered to be linked to seasonal changes in the structure and biochemistry of forest canopies and their relationship with belowground processes (Saleska and others 2003).

In wet tropical forests, dry season increases in latent energy fluxes and evapotranspiration (ET) have long been observed across multiple sites (Shuttleworth 1988; Juarez and others 2007). However, the sustained or increased dry-season gross primary productivity (GPP) has only more recently been observed in site data from the Brazil Flux eddy covariance network (Carswell and others 2002; Saleska and others 2003; Goulden and others 2004; Keller and others 2004). Sustained dry-season GPP is considered possible because of deep soil and root profiles that maintain access to water at depths beyond 10 meters (Nepstad and others 1994). At the same time, dry-season increases in remotely sensed LAI and the Enhanced Vegetation Index (EVI) suggest seasonality in maximum photosynthetic capacity and fraction of photosynthetically active radiation (FPAR) (Huete and others 2006; Myneni and others 2007).

An improved understanding of the mechanisms responsible for tropical forest seasonality is required to evaluate how these ecosystems will respond to drought and future climate fluctuations. DGVMs and Land-Surface Models (LSM) generally do not represent these seasonal dynamics very well because of a general shortage of field data, as well as uncertainty related to canopy structural and biochemical processes (Saleska and others 2003; Ichii and others 2007). Here, we evaluate the sensitivity of seasonal biogeochemistry to soil depths as well as to various canopy phenology schemes using the LPJmL-DGVM (Sitch and others 2003; Bondeau and others 2007). We compare process-based simulations of monthly GPP to independent estimates for GPP derived from MODIS. First, we briefly review the literature on the proximate causes responsible for seasonal phenology and then review field observations and existing modeling approaches used for estimating soil and root profiles in the tropical Amazon. Within the LPJmL-modeling framework we implement four simulation combinations representing various soil depth and phenology modifications. This multi-factorial approach allows us to partition the relative importance of below- and aboveground processes and their influence on tropical ecosystem seasonality represented by GPP fluxes.

## Seasonal Canopy Processes in the Wet Tropics

The primary challenge to modeling seasonality of tropical canopy dynamics stems from uncertainty in the understanding of potential mechanisms responsible for leaf turnover. The main divergence in tropical forest canopy development is based on two functional strategies, one where leaf development is continuous (that is, leaf exchanging) and another where leaf development is episodic (Corlett 1987; Reich 1995). In both cases, soil water availability and its role in determining stem to leaf water potentials appears to control the timing of senescence and leaf development (Reich and Borchert 1984). The recent satellite observations of tropical canopy development suggest an alternative to this perspective, with a flushing of new leaves around the onset of the dry season when soil moisture deficits begin to increase (Elliot and others 2006).

To explain the dry-season increase in LAI and new leaf production it has been proposed that water stress might be alleviated by root access to deep soil water storage (Huete and others 2006). Without seasonal soil moisture stress (because of year-round access to water), seasonal canopy development tracks the next limiting environmental factor, solar

radiation (Elliot and others 2006; Myneni and others 2007; Rivera and others 2007; Stöckli and others 2008). Support for this argument comes from the MODIS remotely sensed LAI, which appears to increase earlier than photosynthetically active radiation (PAR) acting in an 'anticipatory response' to increasing light levels (Myneni and others 2007). Structurally, young leaves have higher photosynthetic or maximum carboxylation capacity (Reich 1995) and so photosynthetic capacity would be maximized to coincide with higher levels of PAR (Rivera and others 2002).

In most ecosystem models, the lack of a generalized theory for wet tropical canopy dynamics has led to simplified tropical phenology schemes based on either water-limitation approaches or assuming no seasonality (Botta and others 2000; Sitch and others 2003; Cox and others 2004; Arora and Boer 2005; Stöckli 2008). However, recent satellite data have begun to constrain the spatial extent, onset, and magnitude of the seasonal cycle of tropical canopies and various dynamic phenology schemes are now being evaluated (Doughty and Goulden 2008; Stöckli 2008). There still remains large observational uncertainty in the remote sensing data that could contribute to enhanced estimates of intra-annual canopy dynamics because of the seasonality of atmospheric contamination that decreases LAI estimates in the wet season (Kobayashi and Dye 2005; Myneni and others 2007). In addition, direct field measurements of LAI show contrasting seasonal canopy dynamics compared to remote sensing, with some sites having little to no seasonality (Carswell and others 2002; Senna and others 2005; Doughty and Goulden 2008). This uncertainty could have a large effect on models that require LAI remote sensing input, for example, CASA (Field and others 1998), as it may contribute to overestimating the seasonal amplitude of tropical forest GPP. Consequently, tropical phenology schemes based on remote sensing should be evaluated within the context of multiple ecosystem processes proposed for sustaining dry-season biogeochemistry.

### Drivers of Aboveground Seasonality Through Belowground Processes

The discovery of roots up to 18 meters deep under wet tropical forests by Nepstad and others (1994) has driven much of the current understanding of tropical dry-season metabolism (Saleska and others 2007). These observations of belowground processes have recently been modified to include hydraulic lift as an additional mechanism for dry-season water availability (Oliveira and others 2005b) and successfully incorporated into various DGVMs and land-surface models improving their representation of tropical seasonality (Lee and others 2005; Baker and others 2008). Uncertainty remains, however, because of sparse field observations of soil and rooting depths and the variability of measurements across sites (1–20 meters, Table 1). Among DGVMs, various datasets and assumptions are used to model soil depths and rooting distributions that result from this observational uncertainty (Table 2).

Developing consistent soil depth information across broad spatial scales remains challenging and scaling from field studies to regional or global analyses is problematic in spite of the various meta-analyses that exist (Canadell and others 1996; Schenck and Jackson 2002) and global datasets available (Table 2). The high spatial variability of point measurements of tropical soil texture and depth (de Negreiros and Nepstad 1994; Williams and others 2002) and the large extent of the Amazon make modeling and optimization approaches for estimating tropical soil depths more attractive than comprehensive field sampling (Ichii and others 2007). These optimization approaches have constrained tropical root depths to 1–10 meters based on estimates of GPP or based on model correlations with remotely sensed vegetation indices, for example, the EVI (Ichii and others 2007).

## Methods

### Study Design

LPJmL is a process-based ecosystem model that simulates daily carbon and water fluxes through photosynthesis and transpiration for nine plant functional types (PFT). At annual time-steps, carbon is allocated to above- and belowground pools and the PFT composition adjusted based on vegetation dynamics and competition for light and water. LPJmL has been comprehensively evaluated and performs well across biomes and at global scales (Sitch and others 2003).

We take a factorial approach to evaluate candidate processes for model improvement to identify the relative importance of processes required for representing drought sensitivity of tropical forests. We focus on belowground processes related to water availability and aboveground processes related to photosynthesis and then evaluate the model using remotely sensed data along a gradient representing changes in precipitation and temperature for 12 field sites (Figure 1 and Table 1). These form part of larger regional and global networks

**Table 1.** List of Field Sites Where Flux Data and MODIS Datasets were Retrieved and LPJmL Simulations were Conducted

| Site ID | Site name | Latitude/Longitude | Vegetation type | DSL | Rooting depth (m) | References |
|---|---|---|---|---|---|---|
| 1 | São Gabriel da Cachoeira | 0° 12′ 35.99″ N 66° 45′ 36″ W | Evergreen broad-leaf forest | 0.6 | No data | No peer-reviewed papers |
| 2 | Manaus KM14 | 2° 35′ 23.99″ S 60° 12′ 36″ W | Evergreen broad-leaf forest | 2.1 | Also see KM34 | (Fan and others 1990) |
| 3 | Manaus KM34 | 2° 36′ 35.99″ S 60° 12′ 36″ W | Evergreen broad-leaf forest | 2.1 | 8–10 | (Fan and others 1990, Malhi and others 1998) |
| 4 | Caxiuanã Forest-Almeririm | 1° 43′ 11.99″ S 51° 27′ 36″ W | Evergreen broad-leaf forest | 3.8 | 10 | (Carswell and others 2002, Fisher and others 2006) |
| 5 | Rebio Jaru Forest, Ji Paraná (Tower A) | 10° 4′ 48″ S 61° 55′ 47″ W | Evergreen broad-leaf forest | 4.5 | >3 | (Grace and others 1995, Von Randow and others 2004) |
| 6 | Sinop Mato Grosso | 11° 24′ 36″ S 55° 19′ 47″ W | Evergreen broad-leaf forest | 5.3 | Sufficient | (Vourlitis and others 2008) |
| 7 | Santarem KM 67 | 2° 51′ 35″ S 54° 57′ 36″ W | Evergreen broad-leaf forest | 5.4 | >4–12 | (Saleska and others 2003, Rice and others 2004) |
| 8 | Bananal Island | 9° 49′ 12″ S 50° 9′ 35″ W | Evergreen broad-leaf forest | 5.5 | No data | No peer-reviewed papers |
| 9 | São Paulo Cerrado (Pé-de-Gigante Reserve) | 21° 37′ 12″ S 47° 38′ 59″ W | Evergreen broad-leaf forest | 5.9 | 2.5 | (da Rocha and others 2002) |
| 10 | Atlantic Forest/São Paulo | 23° 19′ 47″ S 45° 5′ 24″ W | Evergreen broad-leaf forest | 6.0 | NA | No peer-reviewed papers |
| 11 | Brasilia Campo Sujo Bienal Tardia | 15° 56′ 59″ S 47° 52′ 11″ W | Savanna | 6.3 | >1–7 | (Oliveira and others 2005a) |
| 12 | Brasilia-Reserva Ecol Aguas Emendadas | 15° 33′ 0″ S 47° 36′ 0″ W | Woody savanna | 6.5 | >4 | (Miranda and others 1997) |

*Reference indicates relevant studies describing soil and rooting depths as well as observations for seasonal phenology and/or GPP dynamics. The vegetation type refers to the dominant leaf type and physiognomic group.*

including Brazil Flux and the Earth Observing System Core Validation Network, allowing access to ancillary datasets for model evaluation (see ''Analysis'' section for details).

We summarized the seasonal climate dynamics for each site using data available from the Climatic Research Unit (CRU) at University of East Anglia (New and others 2002), which provides mean monthly temperature, precipitation, and cloudiness from 1901 to 2005 at 0.5 degree spatial resolution (Figure 2). Cloud cover, not available for 2003–2005, was estimated using a localized regression related to monthly precipitation and temperature and then converted to photosynthetic active radiation (PAR) using empirical relationships between latitude, day of year, and temperature following methods outlined by Haxeltine and Prentice (1996a). Along the gradient of sites, annual average temperature and precipitation varied from 19 to 27 degrees Celsius and 1.4–3.1 meters, respectively, following primarily changes in latitude.

## Dynamic Phenology Module

To investigate the importance of forest canopy seasonality on GPP, we developed a dynamic phenology

**Table 2.** Soil Depths for Tropical Wet Forests in Amazon from Various DGVMs and Used as Input Data from Global Soil Databases

| Model name | Water access strategy | References |
|---|---|---|
| Biome-BGC | 1–10 m deep soil | (Ichii and others 2007) |
| CASA | Variable with PFT | (Potter and others 2001) |
| CLM | 10 m deep soil | (Lee and others 2005) |
| ED | Uses ISLSCP (see below) | (Moorcroft and others 2001) |
| IBIS | 8 m deep soil | (Costa and Foley 2000) |
| LPJmL (original version) | 1.5 m deep soil<br>2 layers<br>Variable root allocation | (Sitch and others 2003) |
| MOSES/TRIFFED | 3.0 m root depth | (Betts and others 2004) |
| ORCHIDEE | 1.25 m deep soil | (Krinner and others 2005) |
| SiB3 | 3.5 m deep soil | (Baker and others 2008) |
| TEM | 1–2.5 m deep soil | (Vörösmarty and others 1989) |
| **Global soils dataset** | **Soil depth range (for Amazon basin)** | **References** |
| WHRC | <3.0 m | (de Negreiros and Nepstad 1994) |
| FAO | 1.5 m | (Zobler 1986) |
| ISLSCP/GSWP | Wet forests <2.5 m<br>Dry forests 4–5 m | (Webb and Rosenzweig 1993) |
| Inverse modeling | ~4 m | (Kleidon and Heimann 1999) |

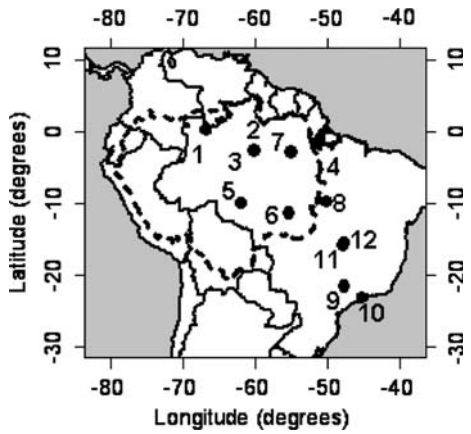


**Figure 1.** Location of study sites (numbers correspond to site ID in Table 1). Dashed boundary represents extent of the Amazon Basin. The increasing dry-season length gradient follows latitude approximately from north to south.

module by relating observed leaf area dynamics to incoming solar radiation and precipitation. These climate variables are considered the primary proximate drivers of tropical leaf area seasonality and we implemented this relationship as a new phenology scheme within the modeling framework of LPJmL. We used remote sensing data to parameterize a logistic model of canopy phenology and to approximate the response of LAI to environmental conditions. Monthly LAI data were obtained from a MODIS Climate Modeling Grid (product MOD15 CMG v4), monthly precipitation from the Tropical Rainfall Measuring Mission (TRMM 3B43v6), and solar radiation from the Clouds and the Earth's Radient Energy System (CERES SFC R4V3) also aboard the TERRA EOS satellite (see Myneni and others (2007) for detailed description of these products). The MODIS Land Cover product, MOD12Q1 (Friedl and others 2002), at 0.50 degree spatial resolution was used to filter non-natural and non-evergreen forest vegetation that might contaminate the LAI signal. To meet these criteria, we removed grid cells with less than 90% broadleaf evergreen cover to eliminate areas with extensive deforestation, forest regrowth or agriculture. The LAI and precipitation data were resampled from 0.25 degrees to 0.50 degrees spatial resolution using bilinear interpolation and the CERES data were downscaled to 0.50 degrees resolution from 1.0 degrees by subdividing the grid cell to four smaller cells with equal solar radiation values.

The filtered LAI and radiation data were then aggregated from individual cell to basin-wide averages following the approach of Myneni and others (2007). The data were then normalized to the maximum of each respective time series resulting in a range between 0 and 1, representing scalars fitting directly into the LPJmL phenology module

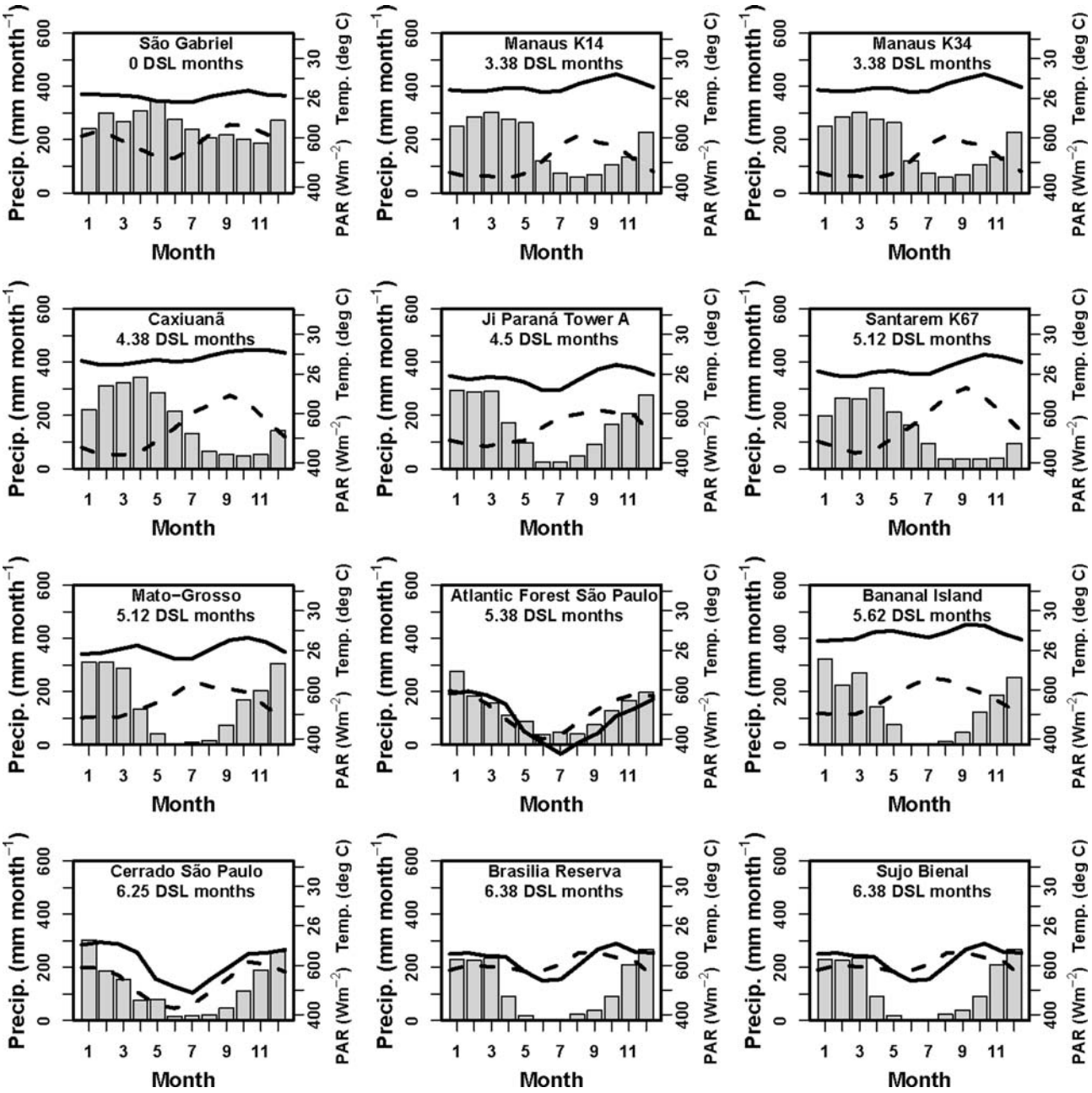


**Figure 2.** Mean monthly climate patterns for the 12 sites (in order of wet to dry sites) averaged over the years 2000–2005 using data from the CRU, which were also used to run the simulations. The solid black line is air temperature, dashed line is photosynthetically active radiation (PAR), and the bars correspond to monthly precipitation.

(described below). The logistic model implemented in LPJmL took the following form based on the notation of Fisher and others (2007);

$$P_R = v_{\min} + v_{\text{amp}} \left( \frac{1}{1 + e^{b - cR_{\text{scalar}}}} \right) \quad (1)$$

where $P_R$ is a radiation-based phenology scalar (ranging between $v_{\min}$ and 1, with 1 representing full canopy), $v_{\min}$ is the minimum annual fraction of LAI and $v_{\text{amp}}$ is its seasonal amplitude. To fit this model, we used normalized monthly radiation as the driver variable ($R_{\text{scalar}}$) and estimated the coefficients $b$ and $c$ for the normalized monthly LAI using a non-linear least squares approach with the Gauss-Newton method.

Because we observed that the sensitivity of LAI to solar radiation generally decreased with decreasing precipitation (Figure 3) we included a co-limitation to represent soil moisture stress and its potential effect on dampening the amplitude of

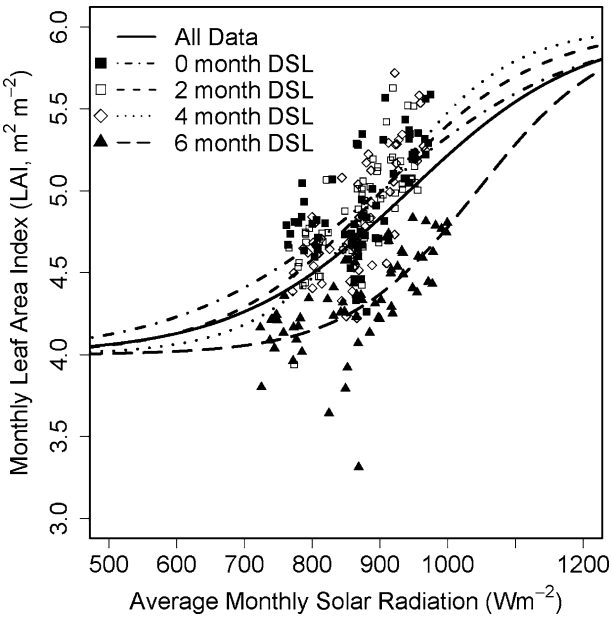


**Figure 3.** MODIS LAI and incoming short wave radiation estimates and non-linear regression model fits for all data and for the corresponding dry-season length (DSL) intervals. The statistical model was fit to normalized MODIS LAI and incoming short wave radiation data. The shortest DSL model fit was used for simulations and in LPJmL after being modified by an additional term to account for water limitation (coefficients and $R^2$ values available in Table 3). Average monthly surface solar radiation was calculated as the monthly maximum of hourly averages following Myneni and others (2007). The figure shows the LAI and radiation data before the normalization procedure.

seasonal leaf area dynamics. This co-limitation was represented by a simple regression model;

$$P_w = S^d \tag{2}$$

where $P_w$ represents water-related stress on phenology based on a soil moisture stress scalar ($S$) as defined in Sitch and others (2003) and $d$ a parameter selected to modify soil moisture as a power function (see Table 3 for $R^2$ values).

This new phenology scheme was implemented in LPJmL for only the tropical evergreen PFT and its LAI dynamics. Within the LPJmL modeling framework, maximum LAI is determined on an annual time step through allometric relationships that distribute carbon from the previous year's GPP to leaves. The fraction of photosynthetic available radiation (FPAR) is then determined daily and related to an individual PFT's daily phenology state. This phenology status is a scalar that is either related to soil moisture or growing degree-days, depending on the PFT requirements. For the tropical evergreen PFT, the original version of LPJmL fixes phenology to be constant throughout the year, therefore, its LAI reflects the maximum value regardless of day of year, soil moisture content or incoming radiation. In the new phenology scheme, to reflect seasonal LAI dynamics for the tropical evergreen PFT, we updated the implementation of the phenology scalar ($P$) so that it was related to radiation ($P_R$) and soil moisture ($P_W$):

$$P = P_R P_W \tag{3}$$

We used the parameters estimated from the LAI and solar radiation model [equation (1)] that were fit to the regions with highest precipitation (Table 3). The scalar, $P_R$, was then weighted by the soil moisture scalar by equation (2). Within LPJmL, $P_R$ was estimated daily by dividing the previous month's radiation (relative to the model simulation date) by the 20-year monthly maximum of radiation. This calculation created a lag response of phenology to radiation by one month rather than a simultaneous response to changing radiation. With this approach, simulated phenology varied according to radiation with a similar sensitivity and amplitude constrained by remote sensing data. We did not implement feedbacks from this seasonal phenology scheme to litter accumulation following leaf fall and we also assumed that carbon was not limiting to leaf area production at the daily time

**Table 3.** Estimated Coefficients from the Logistic Model of Canopy Phenology and Their Corresponding $R^2$ Estimates

| Model | $V_{min}$ | $V_{amp}$ | Radiation scalar | | | Soil scalar |
|---|---|---|---|---|---|---|
| | | | $b$ | $c$ | $R^2$ | $b$ |
| All data | 0.8 | 0.2 | 20.3951 | 21.0619 | 0.294 | 0.01 |
| 0–2 months | | | 30.8423 | 32.1725 | 0.546 | |
| 2–4 months | | | 15.0268 | 16.1084 | 0.369 | |
| 4–6 months | | | 17.8191 | 18.5898 | 0.537 | |
| 6–12 months | | | 9.9534 | 11.3046 | 0.452 | |

*The function was fit to normalized LAI and radiation following division by their corresponding maximum values.*

scale. These processes are important ecologically, but were beyond the current scope of this analysis.

## LPJmL Formulation of GPP

To evaluate the relationship between tropical evergreen leaf area dynamics and modeled carbon fluxes, we investigated the seasonality of photosynthesis because of its direct relationship with LAI and FPAR. Photosynthesis (or GPP) is modeled using a modified Farquhar scheme (Farquhar and others 1980) adapted for global modeling purposes and the PFT concept (Collatz and others 1991). The allocation of leaf nitrogen is assumed to be optimized structurally (that is, within the canopy) and seasonally (Haxeltine and Prentice 1996b) and its distribution is not modeled explicitly. Whole canopy GPP is calculated daily as follows;

$$\mathrm{GPP} = \frac{\left(J_E + J_C - \sqrt{(J_E + J_C)^2 - 4\theta J_E J_C}\right)}{2\theta} \quad (4)$$

where $J_C$ is the Rubisco limited rate of photosynthesis and $J_E$ is the light limited rate of photosynthesis and the empirical shape parameter θ specifies the co-limitation between both terms. $J_E$ is related to APAR (absorbed photosynthetic active radiation, the product of FPAR and PAR), whereas $J_C$ is related to $V_{\mathrm{cmax}}$ (canopy scale maximum carboxylation capacity, μmol $CO_2$ $m^{-2}$ $s^{-1}$) following Haxeltine and Prentice (1996b):

$$J_E = C_1 \mathrm{APAR} \quad (5)$$

$$J_C = C_2 V_{c\max} \quad (6)$$

where $C_1$ and $C_2$ are determined by a variety of photosynthetic pathway parameters as well as the intercellular partial pressure of $CO_2$ ($p_i$) as it is related to atmospheric $CO_2$ and further modified by leaf stomatal conductance (Sitch and others 2003). The value for $V_{\mathrm{cmax}}$ is also related to a series of photosynthetic pathway characteristics and parameters (σ, $b_{C3}$), respiration ($s$), APAR, and θ, also included in equations (4–6).

$$V_{c\max} = \frac{1}{b_{C3}} \frac{C_1}{C_2} ((2\theta - 1)s - (2\theta s - C_2)\sigma)\mathrm{APAR} \quad (7)$$

This equation for $V_{\mathrm{cmax}}$ follows the work of Haxeltine and Prentice (1996b) based on the hypothesis that leaf nitrogen content and Rubisco activity are optimized to vary seasonally and structurally (for a full derivation of $V_{\mathrm{cmax}}$, we refer the reader to publications by Collatz and others (1991), Haxeltine and Prentice (1996b), and Sellers and others (1996)). This optimization is related to extensive evidence that shows photosynthetic enzyme activity increases at high PAR (Haxeltine and Prentice 1996b).

Within this scheme, daily photosynthesis is related directly to LAI by APAR and FPAR. The assimilated carbon is allocated on an annual timestep to four carbon pools with turnover rates specific to each pool (that is, sapwood, heartwood, roots, and leaves). Allocation to LAI is modeled according to a series of allometric rules governed by 'pipe model' theory that maintains each unit of leaf area must be supported by a constant relationship to sapwood area. Following allocation, the allometric rules then determine tree height from sapwood area, then stem diameter, and finally, crown area. These rules are implemented for one average individual tree. Within this framework, maximum LAI is estimated as follows:

$$LAI = \frac{\mathrm{C_{leaf}SLA}}{\mathrm{CA}} \quad (8)$$

where $C_{leaf}$ is the leaf carbon content allocated following one year of GPP, $SLA$ is a PFT determined specific leaf area, and $CA$ is crown area determined by stem diameter (Sitch and others 2003). FPAR is then calculated daily from LAI using Lambert-Beer's Law, where $P$ is the daily phenology scalar that is PFT dependent [from equation (3)] and accounts for the seasonality observed from remotely sensed LAI;

$$\mathrm{FPAR} = \left(1 - \exp(-0.5P \cdot LAI)\right) \quad (9)$$

## Rooting Depth

LPJmL uses a two-layer bucket model to simulate soil hydrology processes following Haxeltine and Prentice (1996a). The soil attributes used in LPJmL include texture (which determines porosity and water holding capacity), thermal diffusivity, and depth (Zobler 1986). The standard version of LPJmL uses a soil depth of 0.5 meters for the upper layer and 1.0 meters for the lower layer and is the same for the entire globe. Roots for each PFT are allocated to the upper and lower soil layer as fractions and the relative distribution of roots determines plant available water with the soil moisture profile representing fast processes (daily rainfall) in the upper layer and slow processes (seasonality) in the lower layer.

The soil depths (at the site level) and rooting profiles (at the PFT level) were adjusted to represent mean basin-wide field conditions (Table 1). Current DGVMs and LSM use a range of approaches to represent soil type. Most commonly, soil depth is

either determined by PFT or set to a fixed value. Most models use soil depths less than 3 meters, as specified by global and regional soil datasets (that is, FAO, GWSP or WHRC; Table 2), which are shallower than observed rooting depths in the Amazon Basin (Nepstad and others 1994; Jipp and others 1998). Only the IBIS model uses depths of 8 meters (for the Amazon Basin), which appears to be more consistent with field observations (Foley and others 2002).

For this analysis we used 8-meter depths for all sites along the precipitation gradient. This depth was more consistent between observations and a recent modeling study (Ichii and others 2007). We did not vary rooting depths along the gradient because there was no consistent pattern across sites from the field studies we reviewed to justify changes in rooting depth (Table 1). We maintained the upper soil depth at 0.5 meters and increased the lower layer thickness to 7.5 meters, which increased the soil water holding capacity. The thickness of the two layers was determined to be consistent with global meta-analyses that demonstrate roots are primarily within 0–1.0 m from the soil surface with a smaller fraction able to access deep water (Canadell and others 1996; Bruno and others 2006). The root distribution fractions were also altered based on a combination of field study results (Canadell and others 1996; Oliveira and others 2005a). Nepstad and others (1994) demonstrated that 75% of dry-season water uptake occurred from depths of 2 meters or greater. For this study, we allocated 55% of the 'tropical evergreen' roots to the upper soil layer (and 45% to the lower layer). For the drought-deciduous PFT (Sitch and others 2003), we allocated 85% of the roots to the upper layer to maintain a competitive advantage for infrequent daily precipitation pulses in drier regions.

## LPJmL Simulations

We ran full 20th century ecosystem simulations using LPJmL (Sitch and others 2003; Gerten and others 2004; Bondeau and others 2007) for each individual site for the four model variations. These variations combined shallow versus deep soils and static versus dynamic canopy phenology, that is, 1.5 meter deep soils and original phenology; 8-meter deep soils and original phenology; 1.5-meter deep soils and seasonal phenology; 8-meter deep soils and seasonal PFT phenology. The monthly CRU data were used as driver data starting in the year 1901 and ending in 2005 (New and others 2002; Österle and others 2003). A spin-up of 1000 years (recycling the first 30 years of climate data, 1901–1930) was applied so that simulated carbon pools could reach equilibrium before the transient climate run began. Vegetation was allowed to develop freely, but the fire disturbance module was disabled. Soil texture was based on input data from FAO (Zobler 1986) with 9 of the 12 sites classified as fine and 3 as medium-coarse texture and all within either the oxisol or gleysol families. Volumetric water holding capacity was only slightly different among these soil texture classes (11% to 15%). Each modeled variable (GPP, LAI, FPAR, $V_{cmax}$, and soil moisture) was output at a monthly time step.

## Analysis

We compared the seasonal cycle of LPJmL leaf area dynamics and GPP to the corresponding site-level data MODIS products. We used the MODIS data assembled by the Oak Ridge National Laboratory's Selected Sites database to calculate monthly mean GPP and LAI from 2000 to 2005. The LAI dataset was filtered with the same quality control filter used by Myneni and others (2007) using results only from the primary algorithm. The data were spatially averaged to 7 km from 1 km pixels ($n = 49$) and then averaged to monthly resolution from approximately 6 years of data. We used a similar method for aggregating monthly data for the MODIS GPP product (also at 1 km resolution) selecting those pixels where the quality control flag was 'very best possible.' MODIS GPP uses a biome specific light-use efficiency model to convert APAR to GPP based on algorithms developed in the BIOME-BGC model (Running and others 2004). The light-use efficiency parameter ($\epsilon$) is dependent on temperature and vapor pressure deficit (VPD) that represent sub-optimal environmental conditions and their constraints on photosynthesis. Water stress is represented by the negative relationship between VPD and stomatal conductance, and also included directly via measurements as FPAR responds to water limitations.

For the comparison with LPJmL, we calculated seasonal anomalies for the LPJmL and MODIS GPP by subtracting the monthly means from the long-term annual mean for the time period 2000–2005. As the MODIS data are 7 km averages and the CRU climate data represent approximately 50 km averages we did not expect the absolute magnitudes to be similar, but the seasonal anomalies should be correlated. The mean monthly anomalies ($n = 12$ months) were compared between the LPJmL modeled and MODIS estimates using the linear

regression technique to calculate $R^2$ and its statistical significance.

## Results

### Phenology Model and Remote Sensing Dynamics

At the basin-scale, the MODIS remote sensing LAI product reproduced the tropical evergreen forest seasonal cycle first noted by Myneni and others (2007). Basin-wide average LAI from MODIS was approximately 4.3 (± 1.3 standard deviations) across all years. The annual cycle of the CERES solar radiation data preceded the basin-wide green-up and the variability in the correlation between LAI and radiation was explained by dry-season length (DSL) (Figure 3). Correspondence between the logistic model of canopy phenology and MODIS LAI estimates were best for the wet sites explaining 54% of the variability (compared to the drier groups where radiation explained 36–45% of the variability). Grouping all the data across DSL reduced the explanatory power of the model to 29% and so by choosing the model coefficients for the wettest site we used the model with the highest predictive power (for coefficients see Table 3). The soil moisture scalar improved the predicted values for the drier sites by gradually reducing the LAI response to radiation where precipitation was lower (Figure 3).

### Annual Ecosystem Dynamics

The LPJmL outputs for GPP, LAI and FPAR were sensitive to the new dynamic phenology and the deep soil depth scenarios. Here, we present the LAI and $V_{cmax}$ dynamics only for the evergreen PFT, which mostly dominated the composition of the wet sites (accounting for up to 75–80% of the PFT coverage). At the drier sites, the dominance of tropical evergreens decreased to 20–30% (and was 0% at the Atlantic Forest São Paulo site because mean annual temperature was too low for this PFT to establish, Figure 2). Tropical rain-green and $C_4$ grasses composed the remaining 15–25% of the PFT composition. At the site level, we present GPP which is integrated over all PFTs in the individual grid cell. Simulated annual GPP ranged from 1800 g C $m^{-2}$ $y^{-1}$ to 2500 g C $m^{-2}$ $y^{-1}$ generally following the gradient of precipitation and dry season, with lower GPP at the drier sites. This value was within the range of observations for Santarem K67 (Saleska and others 2003) but slightly lower than what was reported by Malhi and others (1998) at Caxiuanã. Increasing soil depth stimulated annual GPP by up to 12% in the drier sites whereas the dynamic phenology decreased annual GPP by 16% in the drier sites (Figure 4).

Across sites, LAI ranged between 6 and 8 for the static-phenology simulations and was generally insensitive to changes in soil depth. For the dynamic phenology scenarios, LAI was reduced by 1–2 $m^2$ $m^{-2}$ in the wet season because of imposed radiation limitations and their effect on the developmental state of phenology. $V_{cmax}$ ranged between 30 and 80 μmol $CO_2$ $m^{-2}$ $s^{-1}$ and was lower under the dynamic phenology scenarios reflecting the effect of decreased FPAR in the dry-season. However, the seasonal cycle of $V_{cmax}$ was insensitive to modifications of both phenology and soil depth (Figure 5). Soil moisture dynamics were also insensitive to the dynamic phenology scenarios for both the upper and lower soil layers, and soil moisture in the upper soil layer (0–0.5 meters) did not respond to changes in soil depth. Whereas in the lower soil layer, significant increases in soil water storage during the dry-season were observed (Figure 5).

### Seasonal Ecosystem Dynamics

Seasonality of modeled GPP was observed across all sites and was characterized by an annual amplitude that ranged between ±1 and 4 g C $m^{-2}$ $day^{-1}$ (Figure 4). At the wettest locations (where DSL was $<\sim$5 months) an increase in GPP at the onset of the dry season was observed both from MODIS and LPJmL simulations. This result supports the hypothesis that incoming solar radiation was the primary limiting factor for photosynthesis. Site to site variability for an enhanced dry-season GPP signal increased with dry-season length, with the tropical cerrado forests at Ji Paraná and Mato Grosso showing dry season decreases in GPP across all LPJmL combinations. At the moderately wet sites, sustained dry-season GPP was only attainable under the deep soil scenarios; otherwise the initial dry-season increase in GPP was soon followed by a decrease due to soil moisture stress.

In the moderately wet sites, LPJmL-modeled GPP was strongly correlated with MODIS when the deep soil routine was implemented (Table 4). At the wettest site, São Gabriel, there was no dry-season GPP limitation for the shallow soils because precipitation was sufficiently high throughout the year. At the drier cerrado-savanna sites, the shallow soil routine was adequate for representing the observed seasonal GPP dynamics. The implementation of dynamic phenology did not significantly increase the seasonal pattern of GPP to better

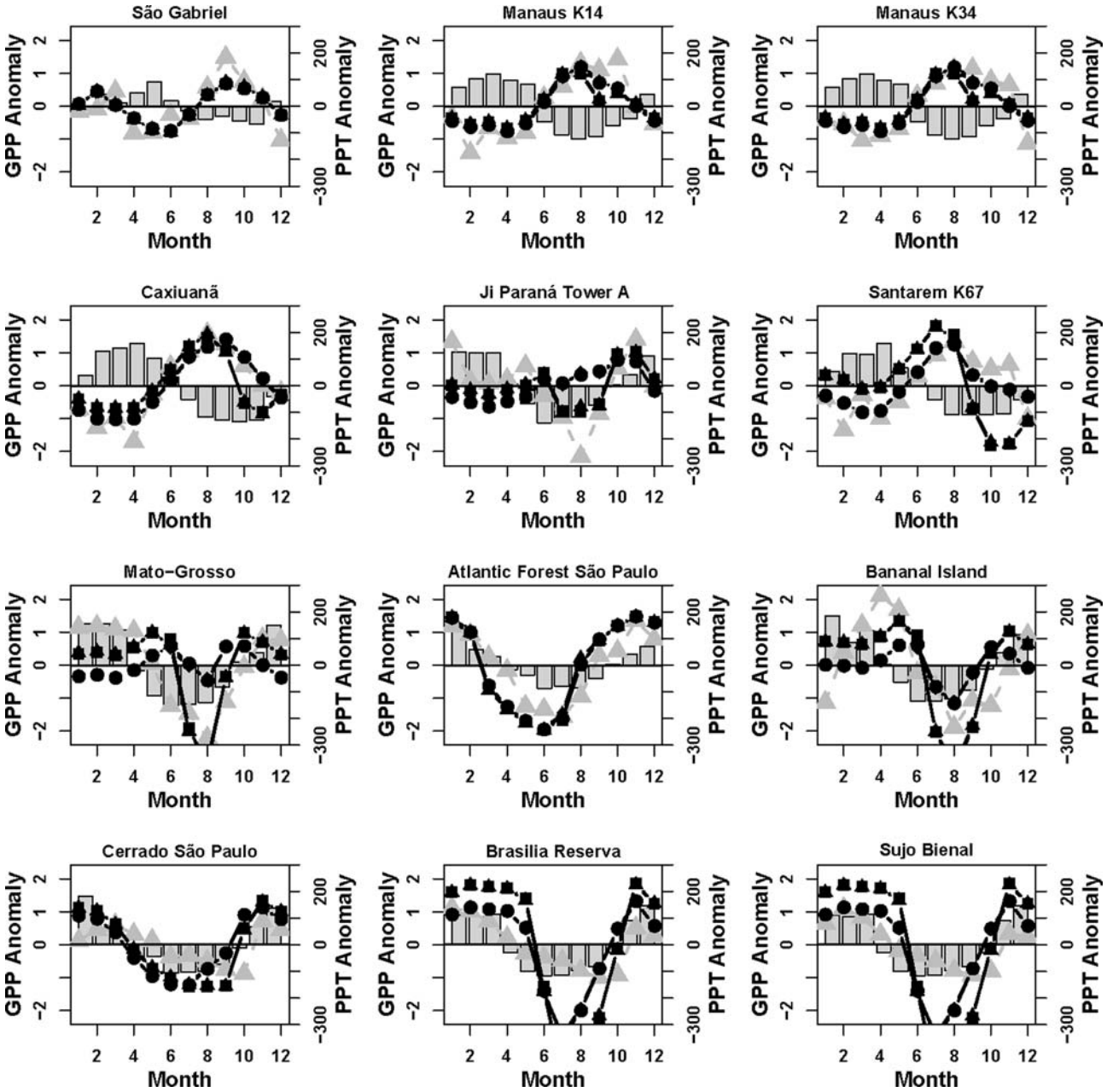


**Figure 4.** Monthly anomalies of modeled site-level gross primary production (GPP, lines), MODIS GPP (*grey triangles*) and precipitation (*bars*). Units are g C $m^{-2}$ $day^{-1}$ for GPP and mm $month^{-1}$ for precipitation. The lines correspond to LPJmL scenarios with black squares (shallow soils and static phenology), black circles (deep soils and static phenology), black triangles (shallow soils and dynamic phenology), and black diamonds (deep soils and dynamic phenology).

match MODIS for any of the wet sites. At the drier sites, the dynamic phenology scheme improved the correlation between LPJmL and MODIS GPP, but only by less than 2%. Although the MODIS GPP estimates are also modeled, we would expect soil water limitations to suppress GPP by reducing dry-season FPAR (one of the inputs for MODIS GPP).

For LAI, the pattern of correlations between LPJmL and MODIS was similar to that of the GPP correlations. The seasonal anomalies were not correlated for the static-phenology scenarios and generally showed higher correlations with the MODIS LAI anomalies for the deep soil scenarios rather than the shallow soil scenarios (Table 4). These correlations were again highest for the wet forest sites and decreased as vegetation shifted toward drier-savanna sites. At the driest sites, the correlation was highest for the deep soil scenario, which was most

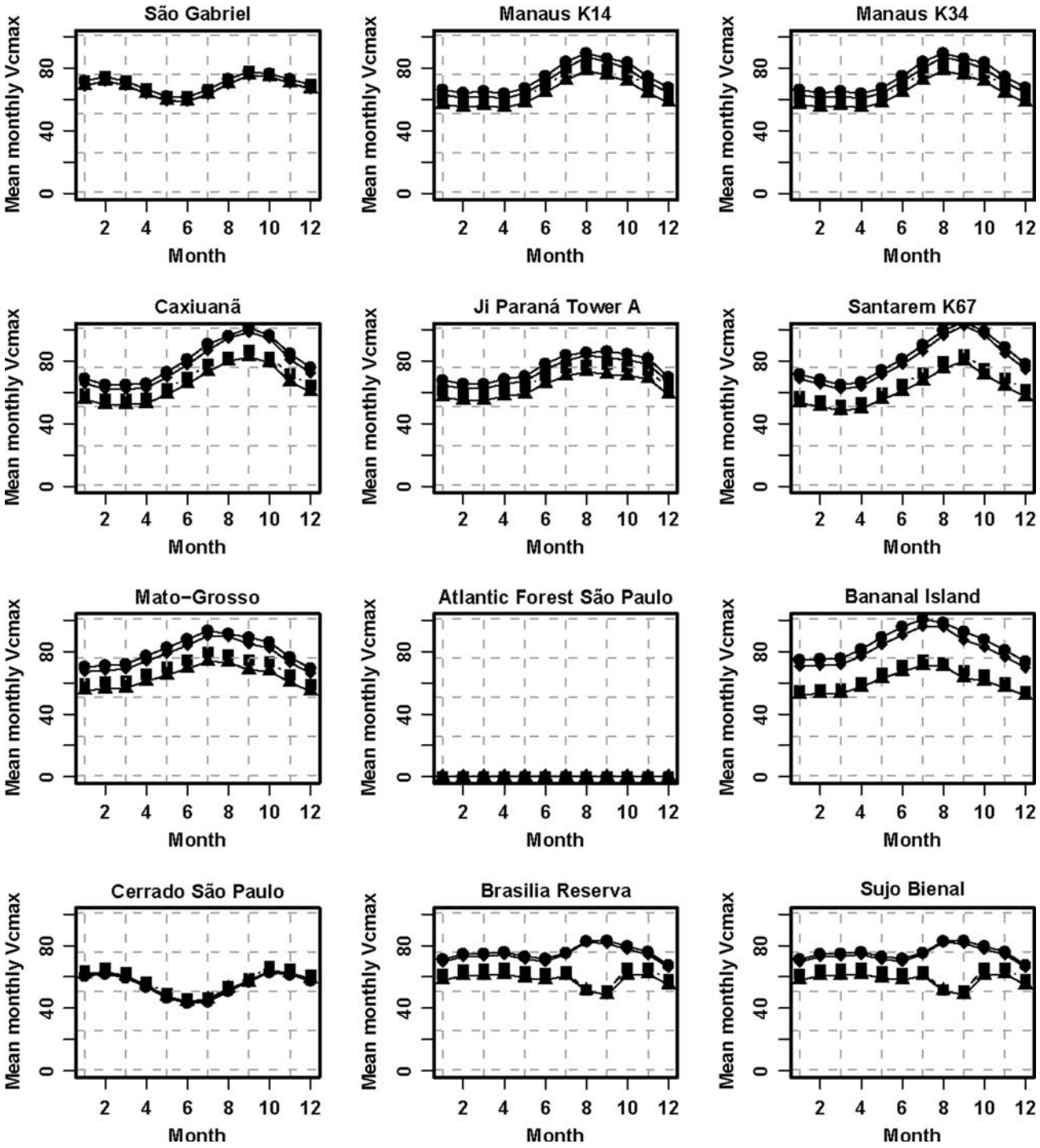


**Figure 5.** Seasonal cycle for tropical evergreen $V_{cmax}$ (*solid lines*). Units are mol $CO_2$ $m^{-2}$ $s^{-1}$ for $V_{cmax}$ and fraction of maximum for soil moisture. Line key as in Figure 4.

likely because the MODIS LAI estimates were influenced by drought tolerant evergreen species.

## $V_{cmax}$ Dynamics

The seasonal cycle of LPJmL-modeled GPP was most sensitive to soil depths rather than to changes in LAI. As the dynamics of LAI (the structural component determining FPAR) did not significantly improve the seasonality of GPP we investigated the role of $V_{cmax}$ seasonality, the key biochemical variable used in the calculation of GPP [equation (4)]. Across all sites $V_{cmax}$ for the tropical evergreen PFT closely followed the seasonality of

**Table 4.** Correlation Coefficients Between LPJmL Simulations and MODIS LAI and GPP Estimates

| Site | LAI | | | | GPP | | | |
|---|---|---|---|---|---|---|---|---|
| | Static phenology and shallow soil | Static phenology and deep soil | Dynamic phenology and shallow soil | Dynamic phenology and deep soil | Static phenology and shallow soil | Static phenology and deep soil | Dynamic phenology and shallow soil | Dynamic phenology and deep soil |
| São Gabriel | 0 n.s. | 0 n.s. | **0.23 n.s.** | 0.23 n.s. | 0.64** | 0.64** | **0.65**** | 0.65** |
| Manaus K14 | 0 n.s. | 0 n.s. | 0.45* | **0.48**** | 0.73** | **0.86**** | 0.74** | 0.86** |
| Manaus K34 | 0 n.s. | 0 n.s. | 0.41* | **0.45*** | 0.72** | **0.84**** | 0.73** | 0.84** |
| Caxiuanã | 0 n.s. | 0 n.s. | **0.26*** | 0.26* | 0.7** | **0.91**** | 0.69** | 0.91** |
| Ji Paraná Tower A | 0 n.s. | 0 n.s. | 0.04 n.s. | 0.13 n.s. | **0.53**** | 0.01 n.s. | 0.53** | 0.01 n.s. |
| Santarem K67 | 0 n.s. | 0 n.s. | 0.18 n.s. | **0.38*** | 0.03 n.s. | **0.66**** | 0.03 n.s. | 0.66** |
| Mato Grosso | 0 n.s. | 0 n.s. | 0.02 n.s. | **0.28*** | 0.49** | 0.08 n.s. | **0.53**** | 0.06 n.s. |
| Atlantic Forest São Paulo | 0 n.s. | 0 n.s. | 0 n.s. | 0 n.s. | 0.79** | **0.79**** | 0.74** | 0.74** |
| Bananal Island | 0 n.s. | 0 n.s. | 0.03 n.s. | 0.07 n.s. | 0.42* | 0.2 n.s. | **0.43*** | 0.22 n.s. |
| Cerrado São Paulo | 0 n.s. | 0 n.s. | **0.25*** | 0.22 n.s. | 0.44* | 0.17 n.s. | **0.46*** | 0.18 n.s. |
| Brasilia Reserva | 0 n.s. | 0 n.s. | 0.1 n.s. | **0.43*** | 0.57** | 0.43* | **0.58**** | 0.44* |
| Sujo Bienal | 0 n.s. | 0 n.s. | 0.02 n.s. | **0.28*** | 0.61** | 0.47** | **0.62**** | 0.48** |

*To determine the significance of $R^2$ the following alpha values were used; P <= 0.001 == **, and P <=0.1 ==*, P =>0.1 ==n.s., for anomalies. In bold is the highest $R^2$ for the original model formulation if the values are equal (that is, shallow and static phenology).*

PAR according to the assumption of optimal resource allocation [equation (7)], resulting in high $V_{cmax}$ during the dry-season. For the scenarios with no dynamic phenology (and therefore no dynamic FPAR), $V_{cmax}$ also increased in the dry-season because of its fundamental relationship with PAR. The deep soil scenarios increased the magnitude of $V_{cmax}$ in the moderately wet sites (Figure 5)—in part because LAI was greater—but also because of a reduction in soil moisture stress causing an increase in stomatal conductance and the internal partial pressure of $CO_2$ (Katul and others 2003). This relationship between $c_i$ and $V_{cmax}$ was strongest at the two sites with lowest precipitation where the dry-season decrease in $V_{cmax}$ was ameliorated with deeper soils (Figure 5). Dynamic phenology slightly affected $V_{cmax}$ by reducing its monthly values because of the reduction in LAI, but there was not a strong effect on the seasonality of $V_{cmax}$ (Figure 5).

## Discussion

### Relative Importance of Soil Depth and Phenology

The results from our experiment are consistent with other modeling studies in that they confirm current soil depths in DGVMs to be underestimated in wet tropical forests to sustain dry-season GPP (Saleska and others 2003; Ichii and others 2007; Baker and others 2008). Here, we show that accounting for deeper soils and the resulting increase in soil water storage is critical for accurately modeling sustained dry-season GPP at moderately wet tropical forest locations (Figure 5). At these locations, where DSL is greater than 3 months, soil moisture limitations gradually become more important as precipitation is unable to recharge soil water losses. At the wettest locations, precipitation is high enough to sustain GPP throughout the year with no water shortage.

The relationship between phenology and seasonal GPP is relatively more complex as we find that structural changes related to LAI are less important than the seasonal cycle of $V_{cmax}$ and its relationship with PAR. The implicit assumption in the LPJmL formulation of $V_{cmax}$ is that nitrogen is allocated optimally throughout the year to coincide with peak solar radiation. The relationship also depends on LAI and FPAR, but because FPAR changes minimally throughout the year, PAR is the primary driver of $V_{cmax}$ dynamics. Across all sites, increasing soil depth (without modifying phenology) improved the correlation between our modeled GPP and MODIS estimates of GPP, whereas the dynamic phenology scheme (with shallow soils) had little to no effect on GPP. The combination of dynamic phenology and deep soils did not consistently improve the correlation between seasonal anomalies. The combination of observational

uncertainty for tropical phenology and the increased complexity to the phenology scheme in LPJmL (by adding the dynamic phenology scheme) does not fully justify a seasonal phenology scheme.

Currently, there is uncertainty regarding the interpretation of remotely sensed observations of tropical forest canopy dynamics. This uncertainty is partly due to possible remote sensing bias and also contradictions between ground and remotely sensed measurements (Senna and others 2005). Uncertainty in distinguishing among proximate drivers and their role in seasonal leaf area dynamics of 'evergreen' tropical forests makes it challenging to model the physiology of canopy dynamics. Our analysis suggests, however, that structural changes in tropical forest canopies (that is, changes in LAI) do not necessarily lead to increases in GPP for two primary reasons. First, the modeled LAI estimates ranged between 5 and 6 $m^2$ $m^{-2}$ or higher and at these levels FPAR is saturated because of its non-linear relation to LAI (from Lambert-Beer's Law, [equation (9)]. Second, the biochemistry of simulated $V_{cmax}$ peaks in the dry season when solar radiation is highest.

These relationships were evident, for example, at the Santarem KM67 site, where mean monthly simulated LAI = 5.4 for shallow soils (5.8 for deep soils), and where we modeled a seasonal amplitude of LAI of approximately 19% (17%) and a corresponding seasonal amplitude of FPAR of 3.5% (2.5%). At lower LAI, the response of FPAR would be more dynamic with presumably a greater seasonal response of GPP. We found that the strong seasonal cycle of $V_{cmax}$, originating from its linear relationship with APAR (Haxeltine and Prentice 1996b) [equation (7)], peaked in the dry season when PAR was greatest. This pattern can be seen clearly in the bimodal peak of $V_{cmax}$ for the São Gabriel site in Figure 5 responding to the spring and autumn equinox. Under dry soil conditions, the response of $V_{cmax}$ to APAR was dampened because of feedbacks on $p_i$ resulting from decreased stomatal conductance. The combination of these effects minimizes the role that a dynamic phenology might have on the seasonality of GPP in wet tropical forests where LAI is high.

The implementation of the Farquhar photosynthesis scheme (Farquhar and others 1980), couples $V_{cmax}$ and soil moisture through their relationship with leaf conductance and internal partial pressure of $CO_2$. The range of estimates modeled by LPJmL for $V_{cmax}$ (Figure 5) were within the estimates found in the literature (Domingues and others 2005), although the seasonality of observed $V_{cmax}$ remains unclear because of field-sampling challenges. Goulden and others (2004) found that light-use efficiency was increased during the dry-season and attributed this change mostly to increases in LAI and possible increases in leaf biochemical capacity resulting from younger leaves. LPJmL simulates canopy-averaged $V_{cmax}$ and simulated values decrease with increasing LAI (as shade leaves increase) and so direct comparisons to field measurements might also be underestimated (Haxeltine and Prentice 1996b). Consequently, the current photosynthesis scheme does not consider diffuse radiation and its positive effects on shade leaf photosynthesis that might result in further underestimation of canopy-integrated GPP. Ichii and others (2007) found similar results with their model that modified photosynthetic capacity by incorporating a seasonal leaf nitrogen allocation function to maximize leaf nitrogen at the end of the dry season. This modification also resulted in increased late dry-season GPP and better correlation with the observational data. It therefore appears that biochemical dynamics rather than structural changes are a secondary mechanism for increases in dry-season metabolism following soil moisture limitation.

## Parameter and Model Structure Uncertainty for Phenology and Soils

The main reason for parameter uncertainty of belowground processes is due to the large size of the Amazon Basin and remote access to field sites. At many sites digging soil pits below several meters is logistically impossible and frequently studies from flux sites conclude that soil moisture is sufficient to prevent any dry-season decrease in GPP, without providing quantitative information on soil depths (Araújo and others 2002; Harris and others 2004). The prevalence of hydraulic lift is also unclear in terms of its variability among species and soil conditions. In a two-layer model, hydraulic lift is less important because the upper layer thickness is large and the process of hydraulic lift mostly affects soil moisture closest to the surface (Lee and others 2005). Determining soil depths by functional types (as done in TRIFFID and CASA (Potter and others 2001; Betts and others 2004)) may be unrealistic under transient climate change because of the assumption that soil depths migrate with species without considering groundwater or impermeable zones.

Beyond field observations, the use of remote sensing indices and their correlation with modeled ecosystem processes represents an alternative for mapping soil depths and calibrating soil parameters (Ichii and others 2007). Remote sensing applications are becoming increasingly reliable as spatial and temporal resolution increase and reduce atmo-

spheric problems encountered in tropical regions. In the meantime, numerical optimization approaches may be most reliable for determining rooting depths (Kleidon and Heimann 1999). These studies conclude that tropical rooting depths are between 8 and 12 meters, although for current regional studies, the application of this approach has been only at coarse spatial scales (550 km cell size).

## Resilience of Amazon Forests to Drought

The proposed mechanisms for the resilience of the Amazon Basin to drought depend on the timescales and intensities of the drought events (Saleska and others 2007). At seasonal to annual timescales, it appears that soil water storage in deep-rooted wet tropical forests is sufficient to sustain dry-season GPP (Figure 4). But the increased water storage is sensitive to recharge from precipitation and as DSL increases to longer than 5–6 months, GPP is suppressed regardless of soil depth (Figure 4).

In the context of the 2005 Amazon drought and projected changes in precipitation from climate change, these results should be interpreted within the timescales during which precipitation changes are taking place. Although the climatic mechanisms may be similar, the 2005 drought was spatially and temporally distinct from climate projections for the year 2100 because of regional variability and the relatively-short duration (Cox and others 2008). The associated 'green-up' during this drought was most likely supported by deep soils and rooting distributions and the changes in EVI correlated to leaf-level biochemical changes or structural changes in FPAR. However, at longer time scales, this analysis suggests that tropical forests will become vulnerable to drought regardless of soil depth because of soil moisture limitations on GPP. Field studies where precipitation inputs have been experimentally reduced at intact tropical forest sites confirm that drought tolerance is temporary and limited to short-timescales (Nepstad and others 2007).

# Conclusion

Recent observations of wet tropical forest dynamics indicate that a dry season increase in GPP is a response of both deep soils and dynamic phenology (Saleska and others 2003). These processes were parameterized into the LPJmL DGVM, which we used to demonstrate that GPP seasonality is most sensitive to soil depths and that changes in canopy structure via LAI have minimal effect on dry-season GPP. For the most part, canopy photosynthesis is regulated by biochemical seasonality (represented by $V_{cmax}$), which is then maintained at higher rates when soil moisture is not limiting. At seasonal time scales, the wet forests of the Amazon may well be light limited but as dry-season length becomes more pronounced soil moisture eventually becomes limiting. DGVMs and land-surface models must accurately represent soil depths at the regional scale while capturing this fine-scale variability.

## Acknowledgments

We acknowledge Marlies Gumpenberger, Fanny Langerwisch, Wolfgang Lucht, Anja Rammig, Paul Stoy, Kirsten Thonicke, and two anonymous reviewers for helpful comments and suggestions. We would like to thank the Distributed Active Archive Center at the Oak Ridge National Laboratory for making the MODIS Selected Sites product available. Funding was provided by the EU Marie Curie Research Training Network GREENCYCLES (MRTN-CT-2004-512464).

## References

Araújo, AC, Nobre AD, Kruijt B, Elbers JA, Dallarosa R, Stefani P, von Randow C, Manzi AO, Culf AD, Gash JHC, Valentini R, Kabat P. 2002. Comparative measurements of carbon dioxide fluxes from two nearby towers in a central Amazonian rainforest: the Manaus LBA site. J Geophys Res 107. doi:10.1029/2001JD000676.

Arora VK, Boer GJ. 2005. A parameterization of leaf phenology for the terrestrial ecosystem component of climate models. Glob Chang Biol 11:39–59.

Baker IT, Prihodko L, Denning AS, Goulden ML, Miller SD, da Rocha HR. 2008. Seasonal drought stress in the Amazon: reconciling models and observations. J Geophys Res 113:G00B01. doi:10.1029/2007JG000644.

Betts RA, Cox PM, Collins M, Harris PP, Huntingford C, Jones CD. 2004. The role of ecosystem-atmosphere interactions in simulated Amazonian precipitation decrease and forest dieback under global warming. Theor Appl Climatol 78:157–75.

Bondeau A, Smith PC, Zaehle S, Schaphoff S, Lucht W, Cramer W, Gerten D, Lotze-Campen H, Muller C, Reichstein M, Smith B. 2007. Modelling the role of agriculture for the 20th century global carbon balance. Glob Chang Biol 13:679–706.

Botta A, Viovy N, Ciais P, Friedlingstein P, Monfray P. 2000. A global prognostic scheme of leaf onset using satellite data. Glob Chang Biol 6:709–25.

Bruno RD, da Rocha HR, de Freitas HC, Goulden ML, Miller SD. 2006. Soil moisture dynamics in an eastern Amazonian tropical forest. Hydrol Process 20:2477–89.

Canadell JG, Jackson RB, Ehleringer JR, Mooney HA, Sala OE, Schulze ED. 1996. Maximum rooting depth of vegetation types at the global scale. Oecologia 108:583–95.

Carswell FE, Costa AL, Palheta M, Malhi Y, Meir P, Costa JdPR, Ruivo MdL, Leal LdSM, Costa JMN, Clement RJ, Grace J. 2002. Seasonality in $CO_2$ and $H_2O$ flux at an eastern Amazonian rain forest. J Geophys Res 107. doi:10.1029/2000JD000284.

Collatz GJ, Ball JT, Grivet C, Berry JA. 1991. Physiological and environmental regulation of stomatal conductance, photo-

synthesis and transpiration: a model that includes a laminar boundary layer. Agric For Meteorol 54:107–36.

Corlett R. 1987. Leaf phenology in tropical trees. Biotropica 31:133–8.

Costa MH, Foley JA. 2000. Combined effects of deforestation and doubled atmospheric $CO_2$ concentrations on the climate of Amazonia. J Clim 13:18–34.

Cox PM, Betts RA, Collins M, Harris PP, Huntingford C, Jones CD. 2004. Amazonian forest dieback under climate-carbon cycle projections for the 21st century. Theor Appl Climatol 78:137–56.

Cox PM, Harris PP, Huntingford C, Betts RA, Collins M, Jones CD, Jupp TE, Marengo JA, Nobre CA. 2008. Increasing risk of Amazonian drought due to decreasing aerosol pollution. Nature 453:212–6.

Cramer W, Bondeau A, Schaphoff S, Lucht W, Smith B, Sitch S. 2004. Tropical forests and the global carbon cycle: impacts of atmospheric carbon dioxide, climate change and rate of deforestation. Philos Trans R Soc Lond 359:331–43.

da Rocha HR, Freitas R, Rosolem R, Juarez RIN, Tannus RN, Ligo MA, Cabral OMR, Silva Dias MAF. 2002. Measurements of $CO_2$ exchange over a woodland savanna (Cerrado *Sensu stricto*) in southeast Brazil. Biota Neotrop 2:1–10.

de Negreiros GH, Nepstad DC. 1994. Mapping deeply rooting forests of Brazilian Amazonia with GIS. Proceedings of ISPRS commission VII symposium—resource and environmental monitoring 7:334–8.

Domingues TF, Berry JA, Martinelli LA, Ometto JPHB, Ehleringer JR. 2005. Parameterization of canopy structure and leaf-level gas exchange for an Eastern Amazonian tropical rain forest (Tapajos National Forest, Para, Brazil). Earth Interactions 9:1–23.

Doughty CE, Goulden ML. 2008. Seasonal patterns of tropical forest leaf area index and $CO_2$ exchange. J Geophys Res 113. doi:10.1029/2007JG000590.

Elliot S, Baker PJ, Borchert R. 2006. Leaf flushing during the dry season: the paradox of Asian monsoon forests. Glob Ecol Biogeogr 15:248–57.

Fan SM, Wofsy SC, Bakwin PS, Jacob DJ. 1990. Atmosphere-biosphere exchange of $CO_2$ and $O_3$ in the Central Amazon forest. J Geophys Res 95:16851–64.

Farquhar GD, von Caemmerer S, Berry JA. 1980. A biochemical model of photosynthetic $CO_2$ assimilation in leaves of $C_3$ plants. Planta 149:78–90.

Field CB, Behrenfield MJ, Randerson JT, Falkowski P. 1998. Primary production of the biosphere: integrating terrestrial and oceanic components. Science 281:237–40.

Fisher JI, Richardson AD, Mustard JF. 2007. Phenology model from surface meteorology does not capture satellite-based greenup estimations. Glob Chang Biol 13:707–21.

Fisher RA, Williams M, Lobo do Vale R, Lola da Costa A, Meir P. 2006. Evidence from Amazonian forests is consistent with isohydric control of leaf water potential. Plant Cell Environ 29:151–65.

Foley JA, Botta A, Coe MT, Costa MH. 2002. El Niño southern oscillation and the climate, ecosystems, and rivers of Amazonia. Global Biogeochem Cycles 4. doi:10.1029/2002GB001872.

Friedl MA, McIver DK, Hodges JCF, Zhang XY, Muchoney D, Strahler AH, Woodcock CE, Gopal S, Schneider A, Cooper A, Baccini A, Gao F, Schaaf CB. 2002. Global land cover mapping from MODIS: algorithms and early results. Remote Sens Environ 83:287–302.

Gerten D, Schaphoff S, Haberlandt U, Lucht W, Sitch S. 2004. Terrestrial vegetation and water balance—hydrological evaluation of a dynamic global vegetation model. J Hydrol 286:249–70.

Goulden ML, Miller SD, da Rocha HR, Menton M, de Freitas HC, Silva Figueira AME, de Sousa CAD. 2004. Diel and seasonal patterns of tropical forest $CO_2$ exchange. Ecol Appl 14:S42–54.

Grace J, Lloyd J, McIntyre J, Miranda AC, Meir P, Miranda HS, Nobre CA, Moncrief J, Malhi Y, Wright I, Gash JHC. 1995. Carbon dioxide uptake by an undisturbed tropical rainforest in southwest Amazonia, 1992–1993. Science 270:778–80.

Harris PP, Huntingford C, Cox PM, Gash JHC, Malhi Y. 2004. Effect of soil moisture on canopy conductance of Amazonian rainforest. Agric For Meteorol 122:215–27.

Haxeltine A, Prentice IC. 1996a. BIOME3: an equilibrium terrestrial biosphere model based on ecophysiological constraints, resource availability, and competition among plant functional types. Global Biogeochem Cycles 10:693–709.

Haxeltine A, Prentice IC. 1996b. A general model for the light-use efficiency of primary production. Funct Ecol 10:551–61.

Huete AR, Didan K, Shimabukuro YE, Ratana P, Saleska SR, Hutyra LR, Yang W, Nemani RR, Myneni RB. 2006. Amazon rainforests green-up with sunlight in dry season. Geophys Res Lett 33:L06405. doi:06410.01029/02005GL025583.

Ichii K, Hashimoto H, White MA, Potter C, Hutyra LR, Huete AR, Myneni RB, Nemani RR. 2007. Constraining rooting depths in tropical rainforests using satellite data and ecosystem modeling for accurate simulation of gross primary production seasonality. Glob Chang Biol 13:67–77.

Jipp PH, Nepstad DC, Cassel DK, de Carvalho CR. 1998. Deep soil moisture storage and transpiration in forests and pastures of seasonally-dry Amazonia. Clim Change 39:395–412.

Juarez RIN, Hodnett MG, Fu R, Goulden ML, von Randow C. 2007. Controls of dry season evapotranspiration over the Amazonian forest as inferred from observations at a Southern Amazon forest site. J Clim 20:2827–39.

Katul G, Leuning R, Oren R. 2003. Relationship between plant hydraulic and biochemical properties derived from a steady-state coupled water and carbon transport model. Plant Cell Environ 26:339–50.

Keller M, Alencar A, Asner GP, Braswell B, Bustamante M, Davidson EA, Feldpausch T, Fernandes E, Goulden ML, Kabat P, Kruijt B, Luizao F, Miller SD, Markewitz D, Nobre AD, Nobre CA, Filho NP, da Rocha HR, Dias PS, Von Randow C, Vourlitis GL. 2004. Ecological research in the large-scale biosphere-atmosphere experiment in Amazonia: early results. Ecol Appl 14:S3–16.

Kleidon A, Heimann M. 1999. Deep-rooted vegetation, Amazonian deforestation, and climate: results from a modelling study. Glob Ecol Biogeogr 8:397–405.

Kobayashi H, Dye DG. 2005. Atmospheric conditions for monitoring the long-term vegetation dynamics in the Amazon using normalized difference vegetation index. Remote Sens Environ 97:519–25.

Krinner G, Viovy N, de Noblet-Ducoudré N, Ogeé J, Polcher J, Friedlingstein P, Ciais P, Sitch S, Prentice IC. 2005. A dynamic global vegetation model for studies of the coupled atmosphere-biosphere system. Global Biogeochem Cycles 19:GB1015. doi:1010.1029/2003GB002199.

Lee JE, Oliveira RS, Dawson TE, Fung IY. 2005. Root functioning modifies seasonal climate. Proc Natl Acad Sci USA 102:17576–81.

Malhi Y, Nobre AD, Grace J, Kruijt B, Pereira MGP, Culf A, Scott S. 1998. Carbon dioxide transfer over a central Amazonian rain forest. J Geophys Res 103:31593–612.

Malhi Y, Roberts JT, Betts RA, Killeen T, Li W, Nobre C. 2008. Climate change, deforestation, and the fate of the Amazon. Science 319. doi:10.1126/science.1146961.

Mayle FE, Power MJ. 2008. Impact of a drier early-mid-holocene climate upon Amazonian forests. Philos Trans R Soc Lond B 363:1829–38.

Miranda AC, Miranda HS, Lloyd J, Grace J, Francey RJ, McIntyre J, Meir P, Riggan P, Lockwood R, Brass J. 1997. Fluxes of carbon, water and energy over Brazilian cerrado: an analysis using eddy covariance and stable isotopes. Plant Cell Environ 20:315–28.

Moorcroft PR, Hurtt GC, Pacala SW. 2001. A method for scaling vegetation dynamics: the ecosystem demography model (ED). Ecol Monogr 71:557–86.

Myneni RB, Yang W, Nemani RR, Huete AR, Dickinson RE, Knyazikhin Y, Didan K, Fu R, Negron Juarez RI, Saatchi SS, Hashimoto H, Shabanov NV, Tan B, Ratana P, Privette JL, Morisette JT, Vermote EF, Roy DP, Wolfe RE, Fiedl MA, Running SW, Votava P, El-Saleous N, Devadiga S, Su Y, Salomonson VV. 2007. Large seasonal swings in leaf area of Amazon rainforests. Proc Natl Acad Sci USA. doi:10.1073/pnas.0611338104.

Nepstad D, De Carvalhos CR, Davidson EA, Jipp PH, Lefebvre PA, Negreiros GH, da Silva ED, Stone TA, Trumbore SE, Vieira S. 1994. The role of deep roots in the hydrological and carbon cycles of Amazonian forests and pastures. Nature 372:666–9.

Nepstad D, Tohver IM, Ray D, Moutinho P, Cardinot G. 2007. Mortality of large trees and lianas following experimental drought in an Amazon forest. Ecology 88:2259–69.

New M, Lister D, Hulme M, Makin I. 2002. A high-resolution data set of surface climate over global land areas. Climate Res 21:1–25.

Oliveira RS, Bezerra L, Davidson EA, Pinto F, Klink CA, Nepstad D, Moreira A. 2005. Deep root function in soil water dynamics in cerrado savannas of central Brazil. Funct Ecol 19:574–81.

Oliveira RS, Dawson T, Burgess SSO, Nepstad D. 2005. Hydraulic redistribution in three Amazonian trees. Oecologia 145:354–63.

Österle H, Gerstengarbe FW, Werner PC. 2003. Homogenisierung und Aktualisierung des Klimadatensatzes der Climate Research Unit der Universität of East Anglia, Norwich. Terra Nostra 6:326–9.

Potter C, Klooster S, de Carvalho CR, Genovese VB, Torregrosa A, Dungan J, Bobo M, Coughlan J. 2001. Modeling seasonal and interannual variability in ecosystem carbon cycling for the Brazilian Amazon region. J Geophys Res 106:10423–46.

Reich PB. 1995. Phenology of tropical forests: patterns, causes, and consequences. Can J Bot 73:164–74.

Reich PB, Borchert R. 1984. Water stress and tree phenology in a tropical dry forest in the lowlands of Costa Rica. J Ecol 72:61–74.

Rice AH, Pyle EH, Saleska SR, Hutyra LR, Palace M, Keller M, de Camargo PB, Portilho K, Marques DF, Wofsy SC. 2004. Carbon balance and vegetation dynamics in an old-growth Amazonian forest. Ecol Appl 14:S55–71.

Rivera G, Elliot S, Caldas LS, Nicolossi G, Coradin VTR, Borchert R. 2002. Increasing day-length induces spring flushing of tropical dry forest trees in the absence of rain. Trees 16:445–56.

Rivera G, Elliot S, Caldas LS, Nicolossi G, Coradin VTR, Borchert R. 2007. Increasing day-length induces spring flushing of tropical dry forest trees in the absence of rain. Trees 16:445–56.

Rödenbeck C, Houweling S, Gloor M, Heimann M. 2003. CO2 flux history 1982–2001 inferred from atmospheric data using a global inversion of atmospheric transport. Atmos Chem Phys 3:1919–64.

Running SW, Nemani RR, Heinsch FA, Zhao M, Reeves M, Hashimoto H. 2004. A continuous satellite-derived measure of global terrestrial primary production. Bioscience 54:547–60.

Salazar LF, Nobre CA, Oyama MD. 2007. Climate change consequences on the biome distribution in tropical South America. Geophys Res Lett 34. doi:10.1029/2007GL029695.

Saleska SR, Didan K, Huete AR, da Rocha HR. 2007. Amazon forests green-up during 2005 drought. Science. doi:10.1126/science.1146663.

Saleska SR, Miller SD, Matross DM, Goulden ML, Wofsy SC, da Rocha HR, de Camargo PB, Crill P, Daube BC, de Freitas HC, Hutyra LR, Keller M, Kirchhoff V, Menton M, Munger JW, Pyle EH, Rice AH, Silva H. 2003. Carbon in Amazon forests: unexpected seasonal fluxes and disturbance-induced losses. Science 302:1554–8.

Schenck HJ, Jackson RB. 2002. Rooting depths, lateral root spreads and below-ground/above-ground allometries of plants in water-limited ecosystems. J Ecol 90:480–94.

Sellers P, Randall DA, Collatz GJ, Berry JA, Field CB, Dazlich D, Zhang C, Collelo GD, Bounoua L. 1996. A revised land surface parameterization (SiB2) for atmospheric GCMs. Part I: model formulation. J Clim 9:706–37.

Senna MCA, Costa MH, Shimabukuro YE. 2005. Fraction of photosynthetically active radiation absorbed by Amazon tropical forest: a comparison of field measurements, modeling, and remote sensing. J Geophys Res 110. doi:10.1029/2004JG000005.

Shuttleworth WJ. 1988. Evaporation from Amazonian rainforest. Proc R Soc Lond 233:321–46.

Sitch S, Smith B, Prentice IC, Arneth A, Bondeau A, Cramer W, Kaplan JO, Levis S, Lucht W, Sykes MT, Thonicke K, Venevsky S. 2003. Evaluation of ecosystem dynamics, plant geography and terrestrial carbon cycling in the LPJ dynamic global vegetation model. Glob Chang Biol 9:161–85.

Stöckli R, Rutishauser T, Dragoni D, O'Keefe J, Thornton PE, Jolly M, Lu L, Denning AS. 2008. Remote sensing data assimilation for a prognostic phenology model. J Geophys Res 113. doi:10.1029/2008JG000781.

Von Randow C, Manzi AO, Kruijt B, de Oliveira PJ, Zanchi FB, Silva RL, Hodnett MG, Gash JHC, Elbers JA, Waterloo MJ, Cardoso FL, Kabat P. 2004. Comparative measurements and seasonal variations in energy and carbon exchange over forest and pasture in South West Amazonia. Theor Appl Climatol 78:5–26.

Vörösmarty CJ, Moore B III, Grace AL, Gildea MP, Melillo JM, Peterson BJ, Rastetter EB, Steudler PA. 1989. Continental scale models of water balance and fluvial transport: an application to South America. Global Biogeochem Cycles 3:241–55.

Vourlitis GL, de Souza Nogueira J, de Almeida Lobo F, Sendall KM, de Paulo SR, Dias CAA, Pinto OB Jr, de Andrade NLR. 2008. Energy balance and canopy conductance of a tropical semi-deciduous forest of the southern Amazon Basin. Water Resour Res 44. doi:10.1029/2006WR005526.

Webb RS, Rosenzweig CE. 1993. Specifying land surface characteristics in general circulation models: soil profile data set and derived water-holding capacities. Global Biogeochem Cycles 7:97–108.

Williams M, Shimabukuro YE, Herbert DA, Lacruz SP, Renno CD, Rastetter EB. 2002. Heterogeneity of soils and vegetation in an eastern Amazonian rain forest: implications for scaling up biomass and production. Ecosystems 5:692–704.

Zobler L. 1986. A world soil file for global climate modeling. NASA Technical Memorandum 87802, 32 pp.